SI Appendix for
"Mapping Global Resource-Driven Nature Loss in the Mining Sector"

Yu-Tong Cheng[1], Nguyen Tien Hoang[1], Yushin Shinoda[2], Kamrul Islam[3], Masaharu Motoshita[3], Taku Kadoya[2], Keiichiro Kanemoto[1,4*]

Contents:

[1]Graduate School of Environmental Studies, Tohoku University, Sendai, Japan.

[2]Biodiversity Division, National Institute for Environmental Studies (NIES), Ibaraki, Japan.

[3]Research Institute of Science for Safety and Sustainability, National Institute of Advanced Industrial Science and Technology, Tsukuba, Japan.

[4]Interdisciplinary Cluster for Cutting Edge Research, Shinshu University, Matsumoto, Japan.

[*]Corresponding author. E-mail: keiichiro.kanemoto@gmail.com

S1. Deforestation Areas for 20 Commodities

Commodity	Area (Km^2)	Proportion (%)
Iron	1046.01	7.16%
Copper	523.89	3.58%
Lead	116.74	0.80%
Zinc	61.41	0.42%
Gold	3183.65	21.78%
Silver	62.94	0.43%
Chromium	17.45	0.12%
Manganese	135.55	0.93%
Molybdenum	168.43	1.15%
Nickel and Cobalt	616.79	4.22%
Tin	84.34	0.58%
Tungsten	11.48	0.08%
Aluminium (Bauxite)	764.71	5.23%
Ilmenite	58.40	0.40%
Lithium	245.95	1.68%
PGE	113.83	0.78%
Uranium	95.73	0.65%
Other metals	196.41	1.34%
Coal	6044.75	41.35%
Other non-metals	1070.57	7.32%
ALL	14619.05	100%

S2. Global Distribution of Mining Areas for 20 Commodities

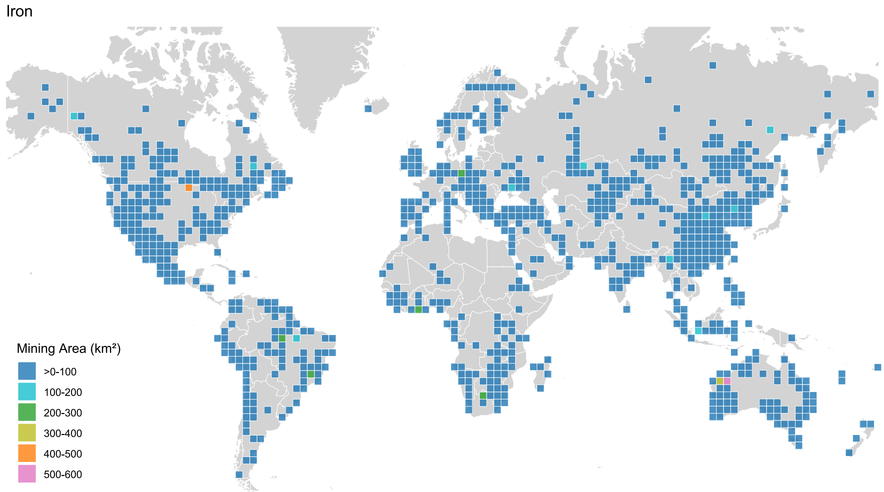

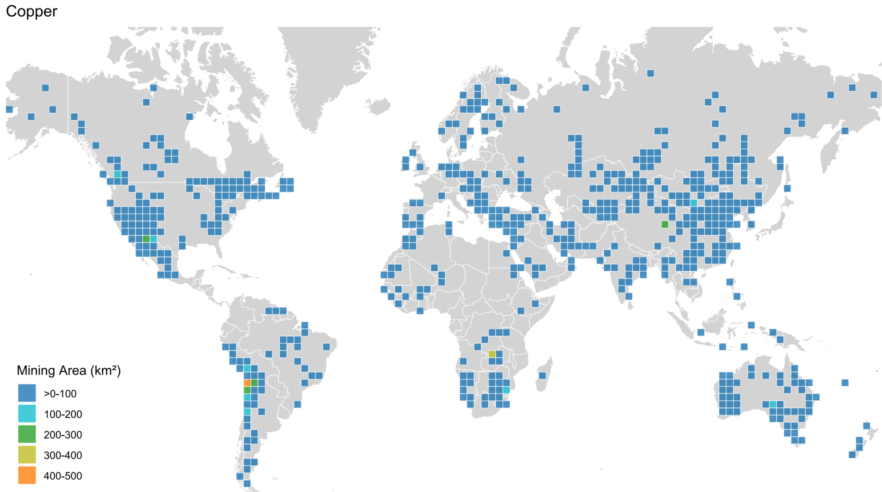

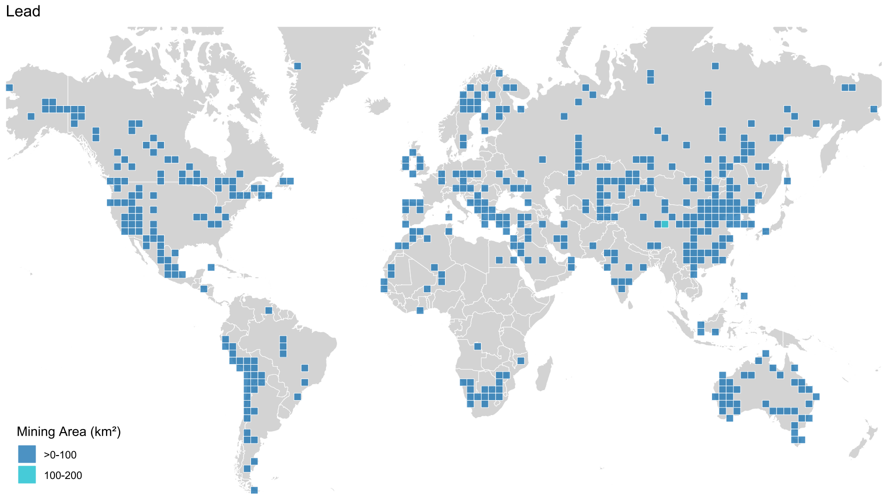

Zinc

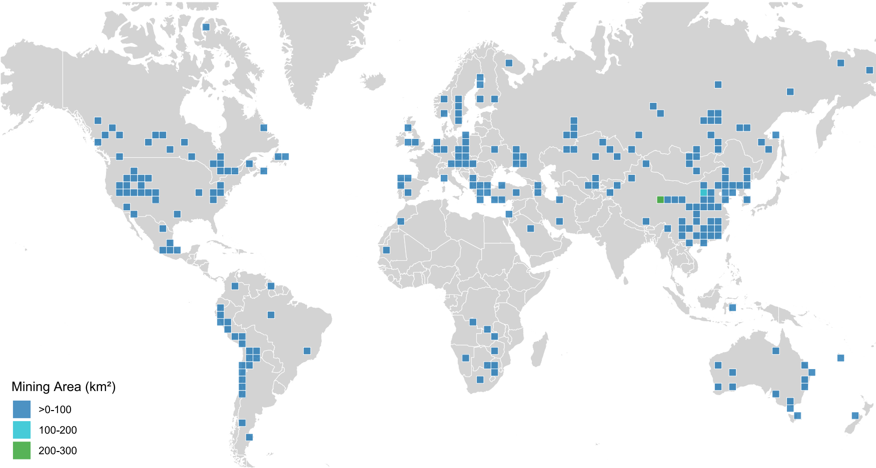

Gold

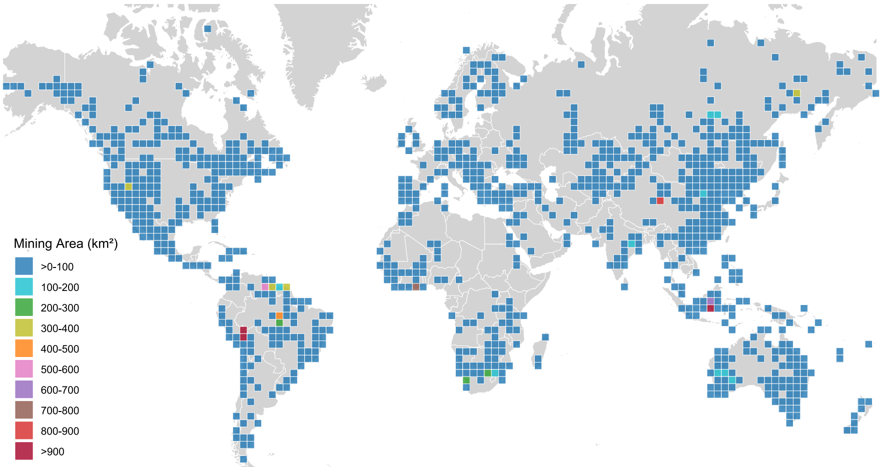

Silver

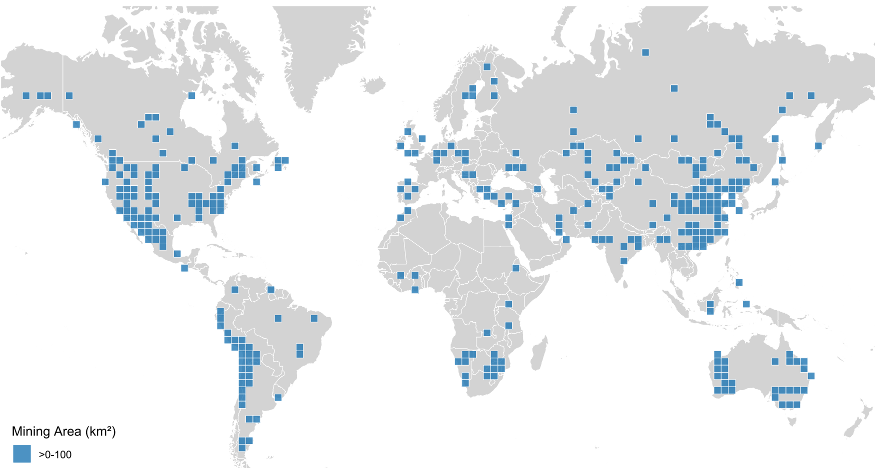

Chromium

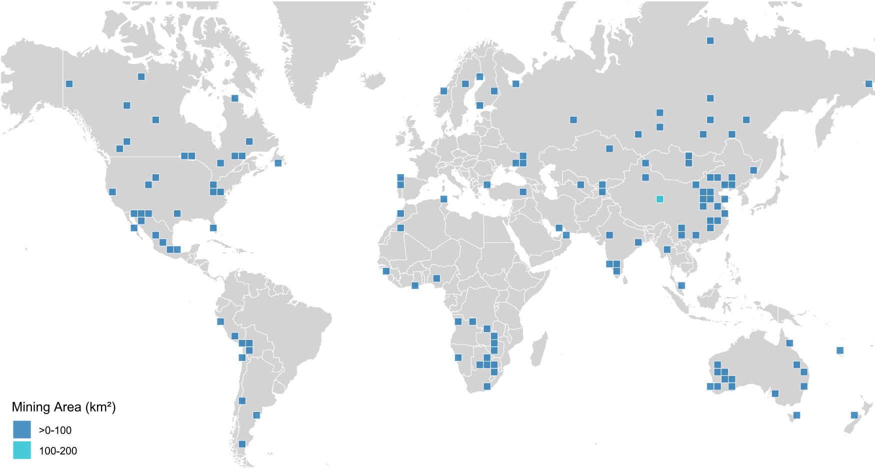

Manganese

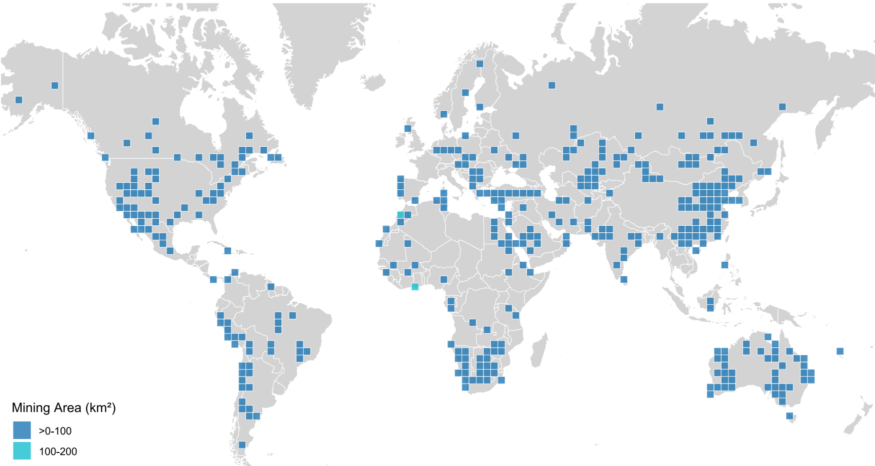

Molybdenum

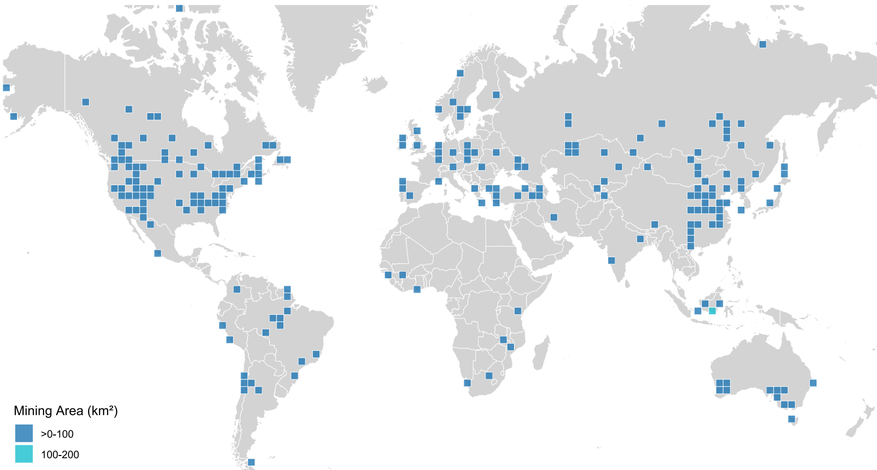

Nickel and Cobalt

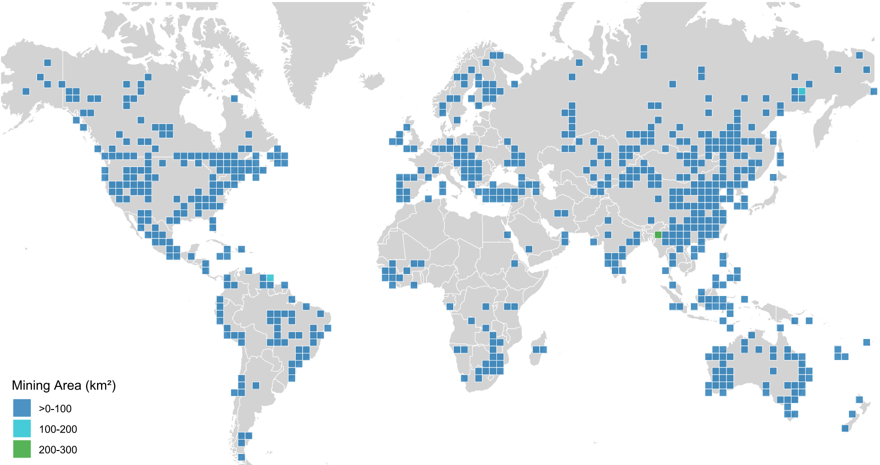

Tin

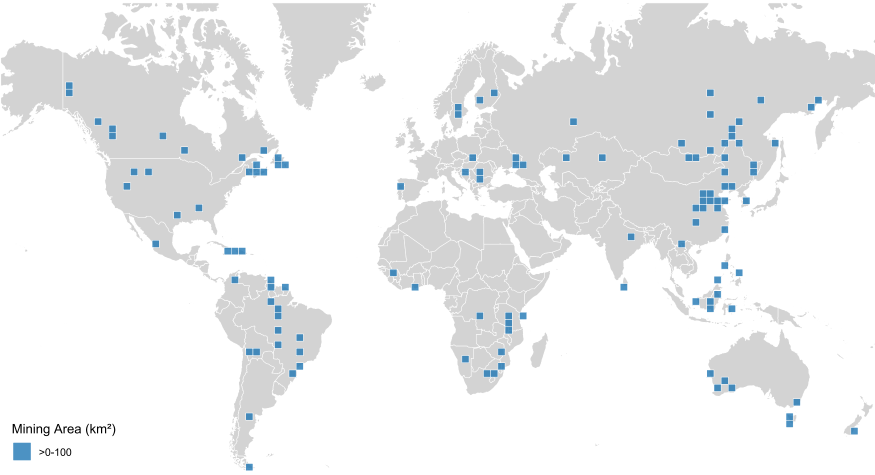

Tungsten

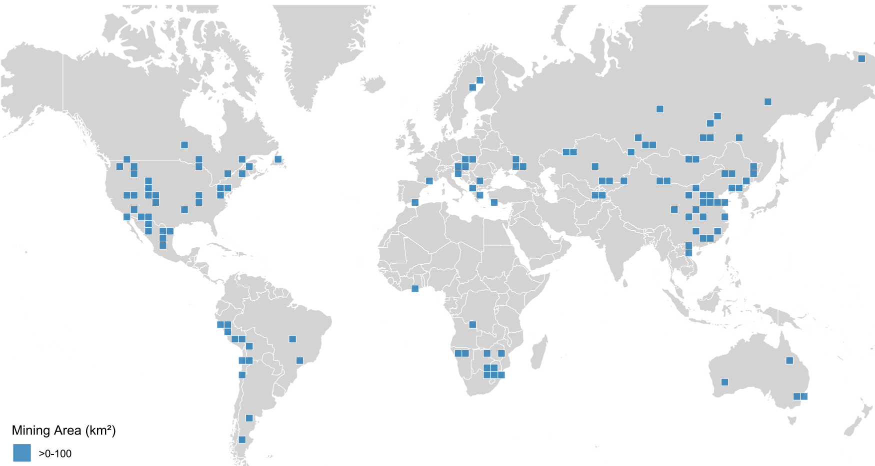

Aluminium (Bauxite)

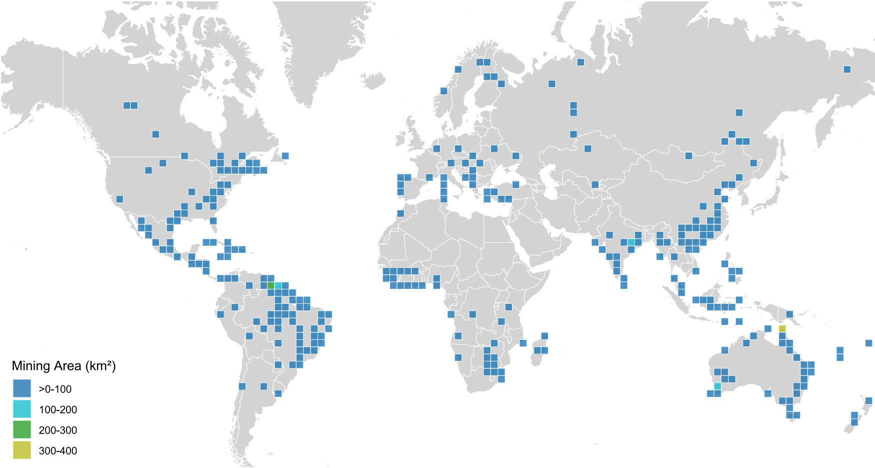

Ilmenite

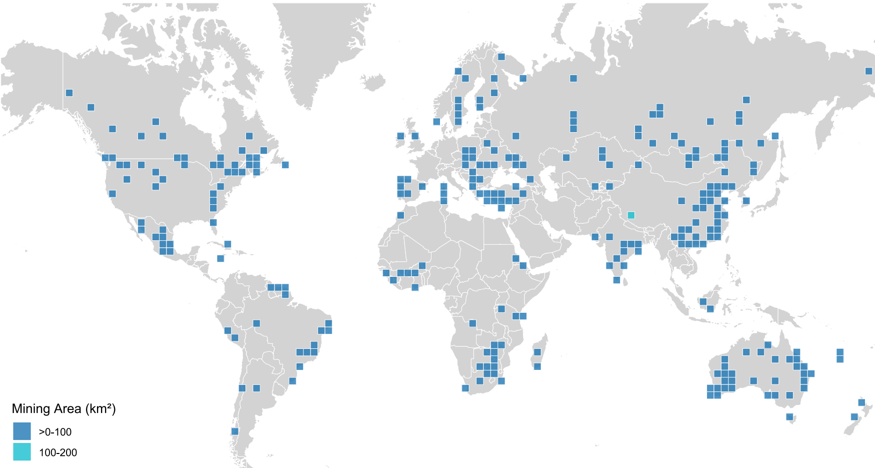

Lithium

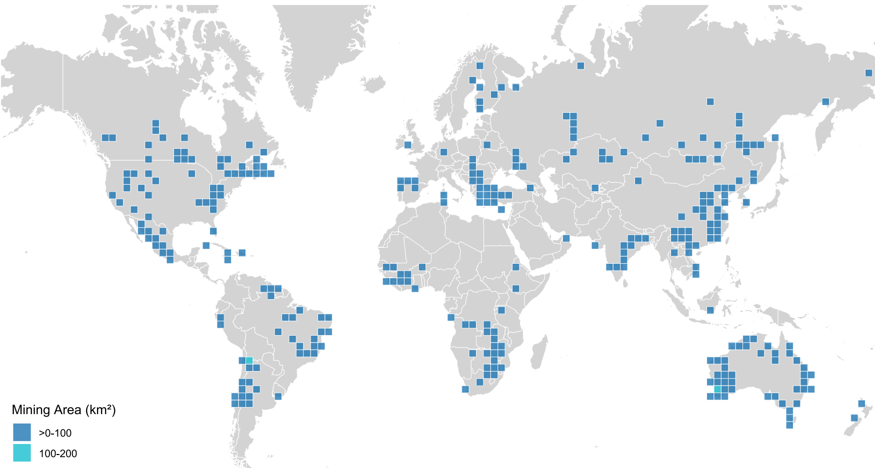

PGE

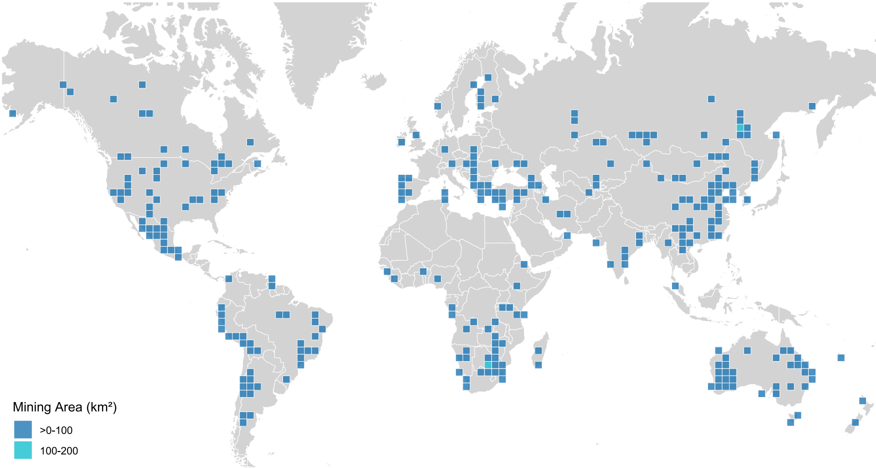

Uranium

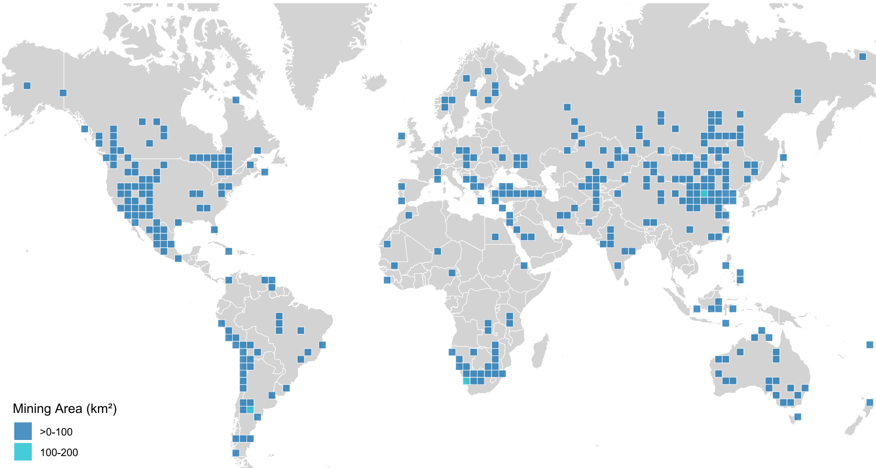

Other metals

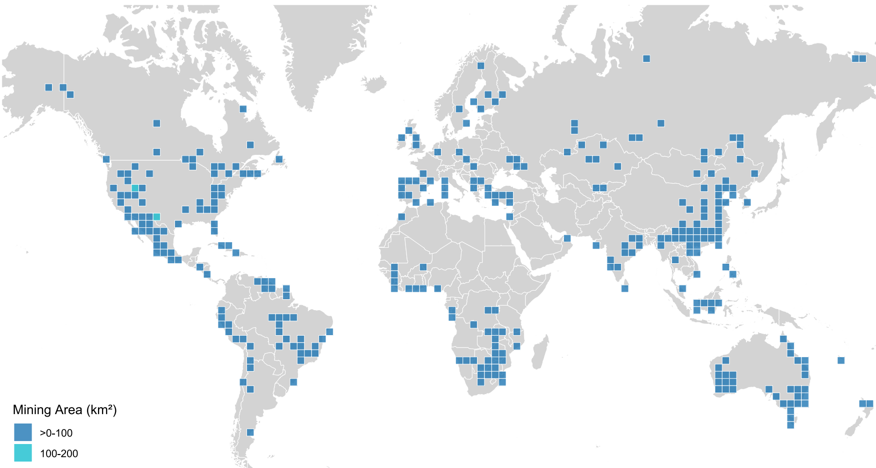

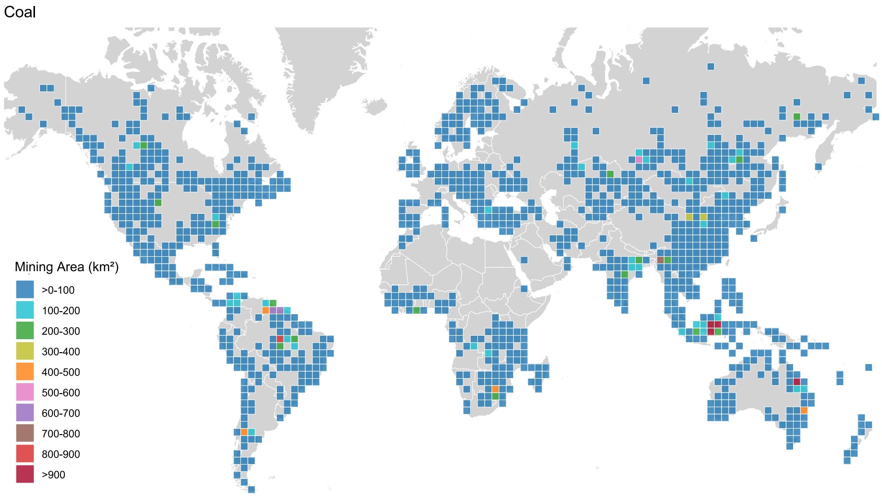
Coal
Mining Area (km²)
>0-100
100-200
200-300
300-400
400-500
500-600
600-700
700-800
800-900
>900

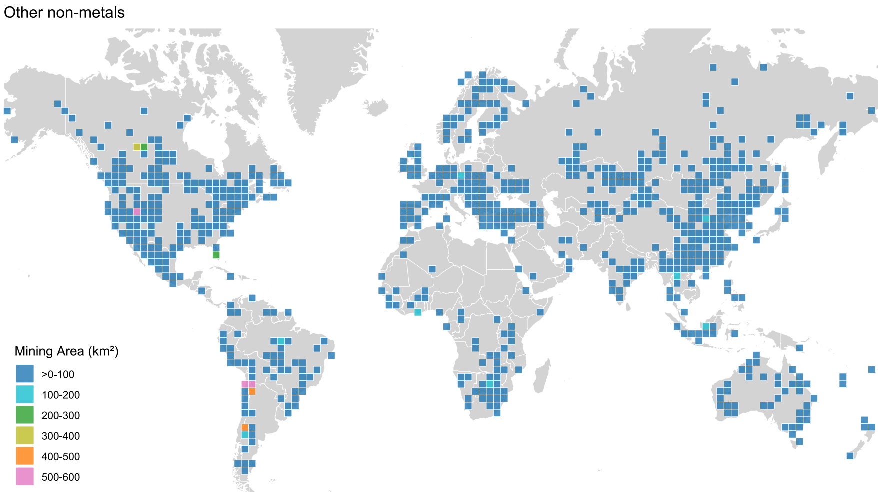
Other non-metals
Mining Area (km²)
>0-100
100-200
200-300
300-400
400-500
500-600

S3. Spatial Variation in Deforestation-to-Mining Area Ratio for 20 Commodities

Iron

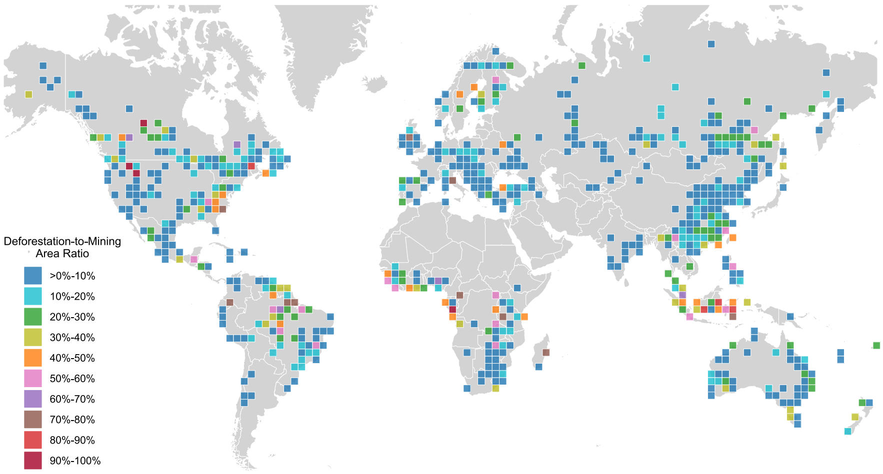

Copper

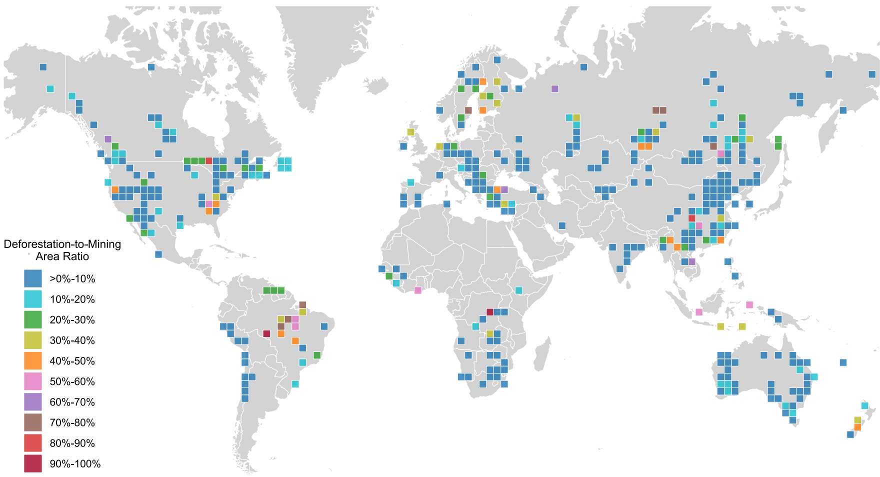

Lead

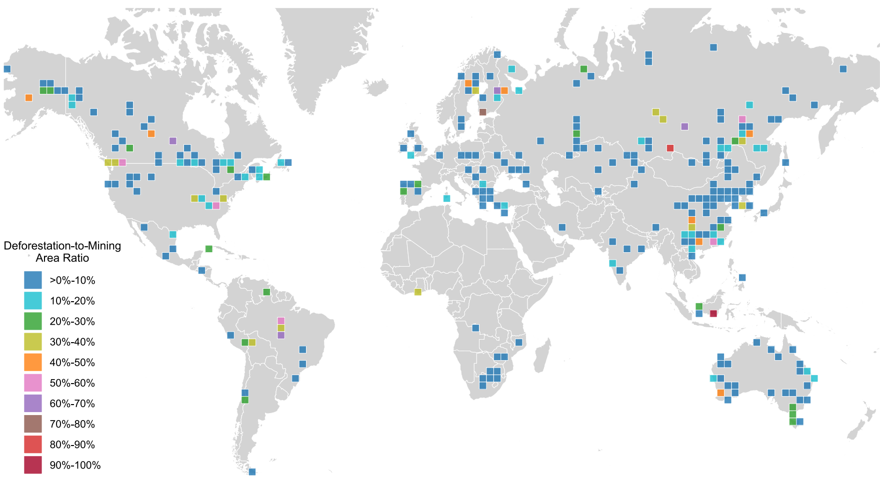

Zinc

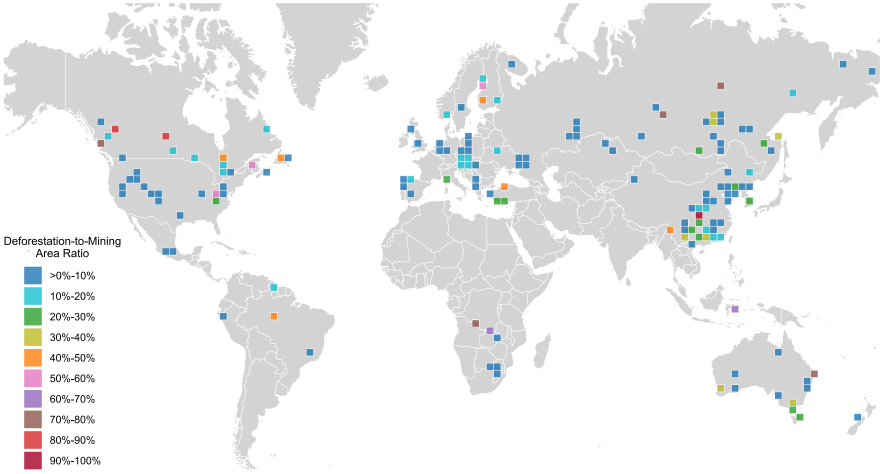

Gold

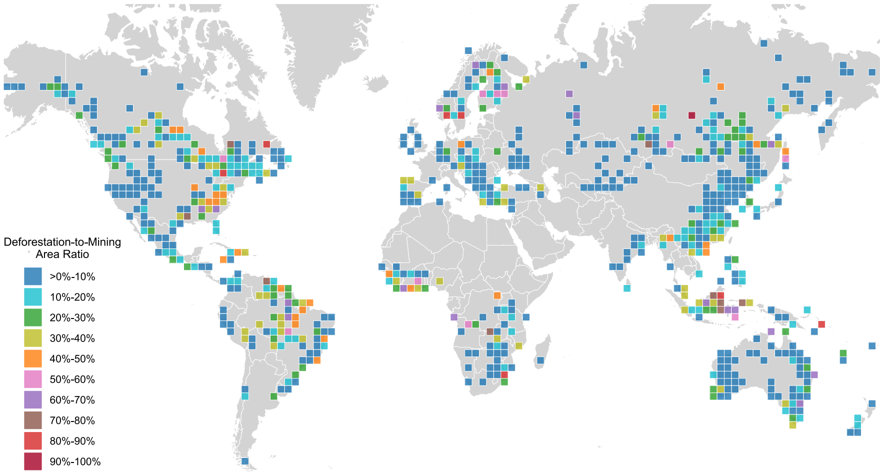

Silver

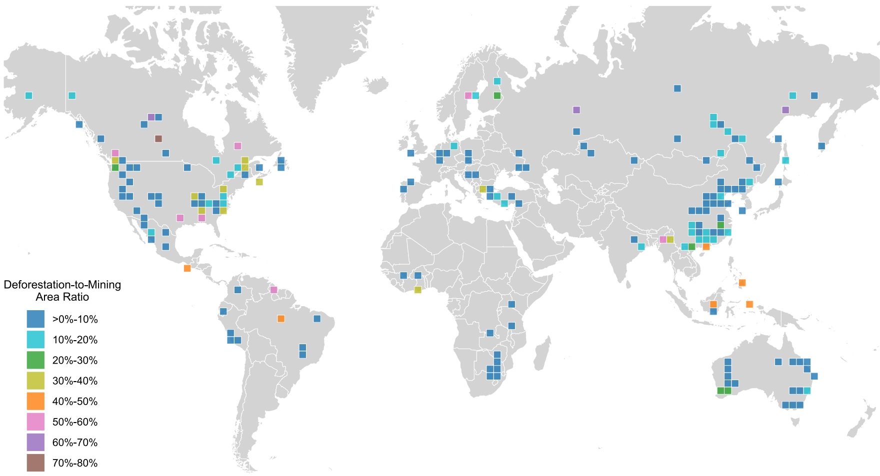

Chromium

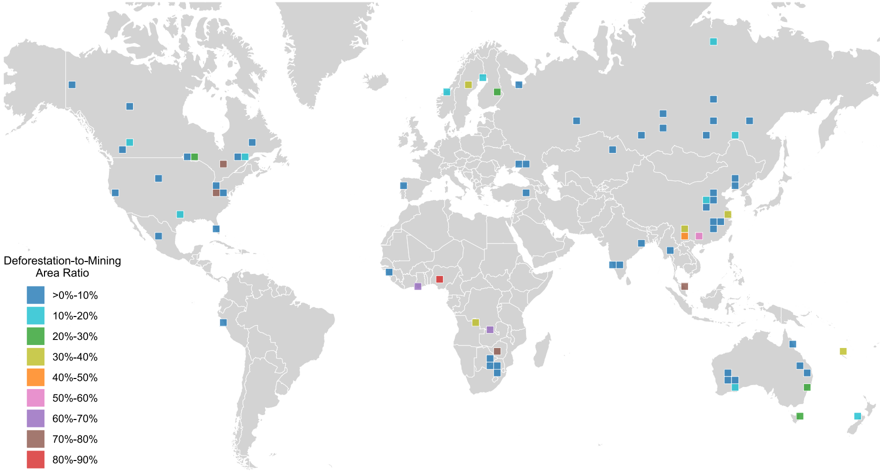

Manganese

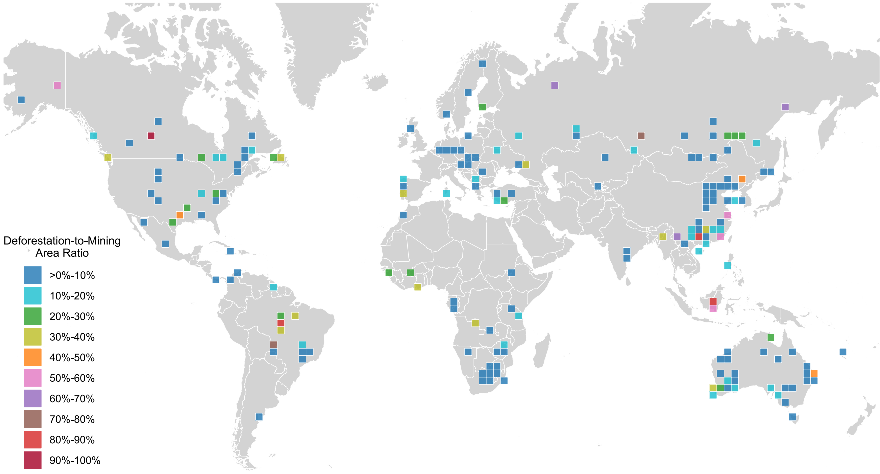

Molybdenum

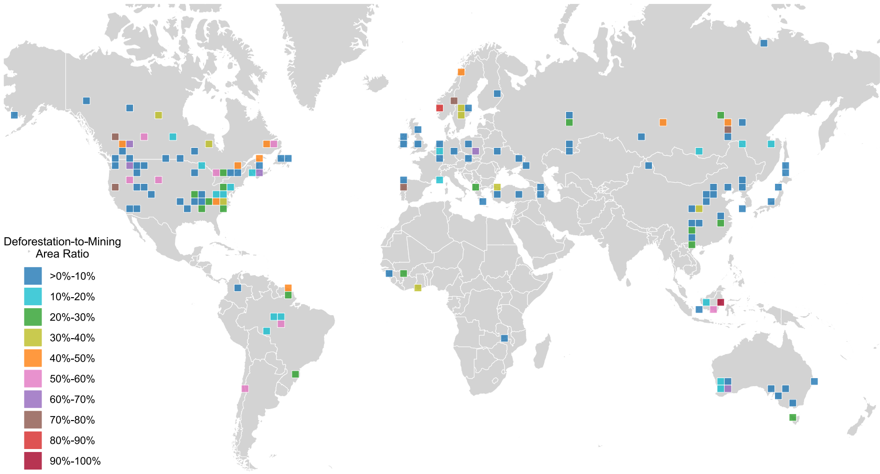

Nickel and Cobalt

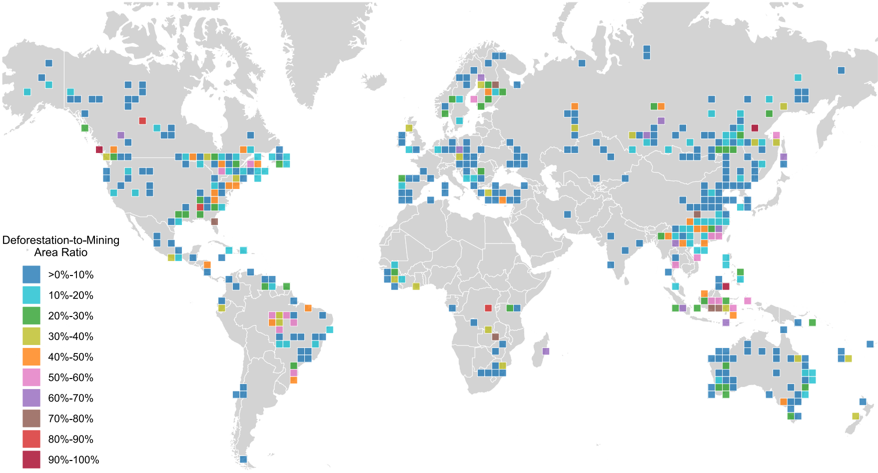

Tin

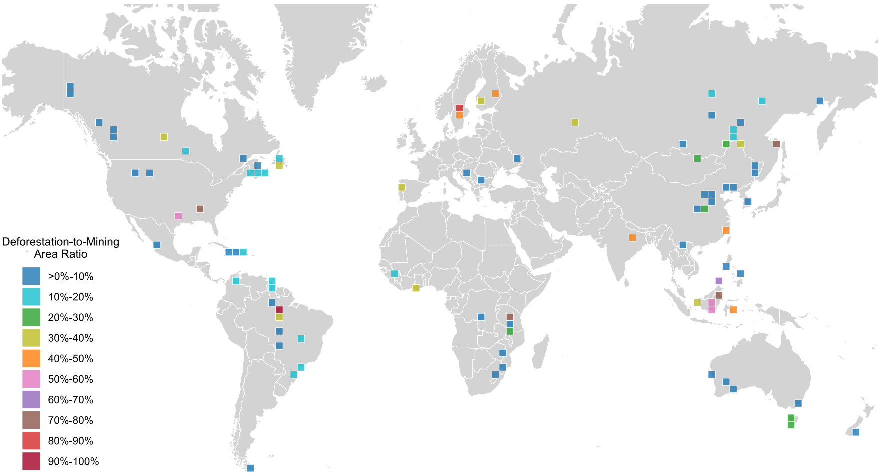

Tungsten

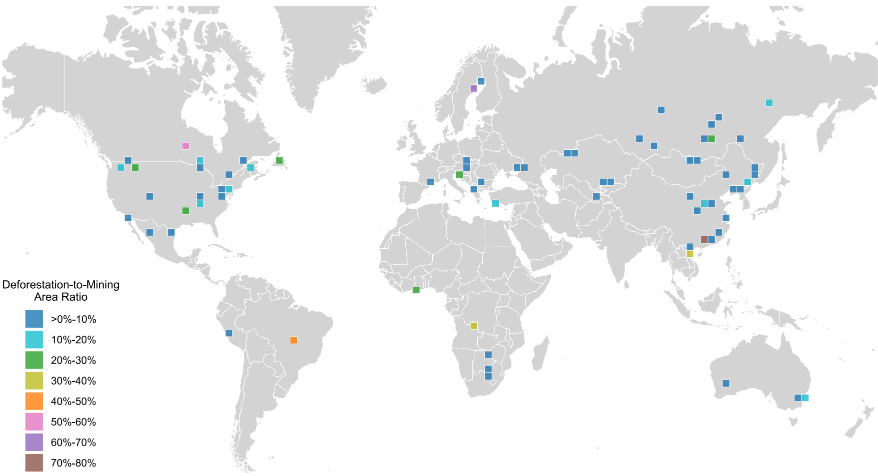

Aluminium (Bauxite)

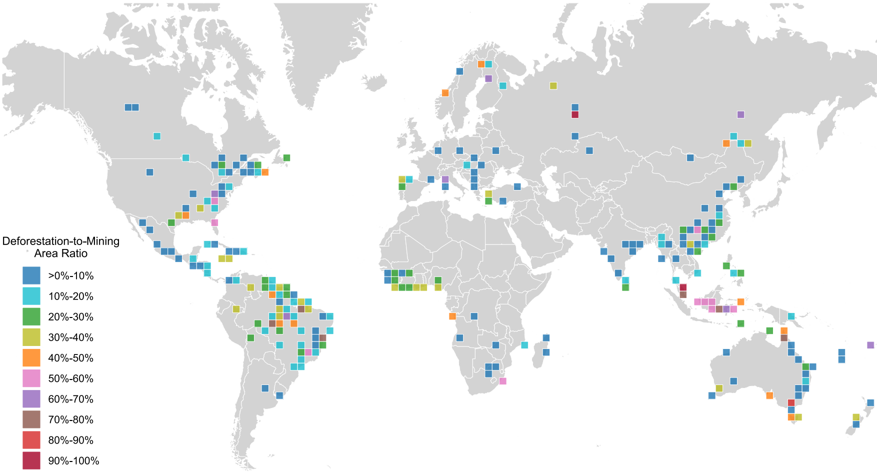

Ilmenite

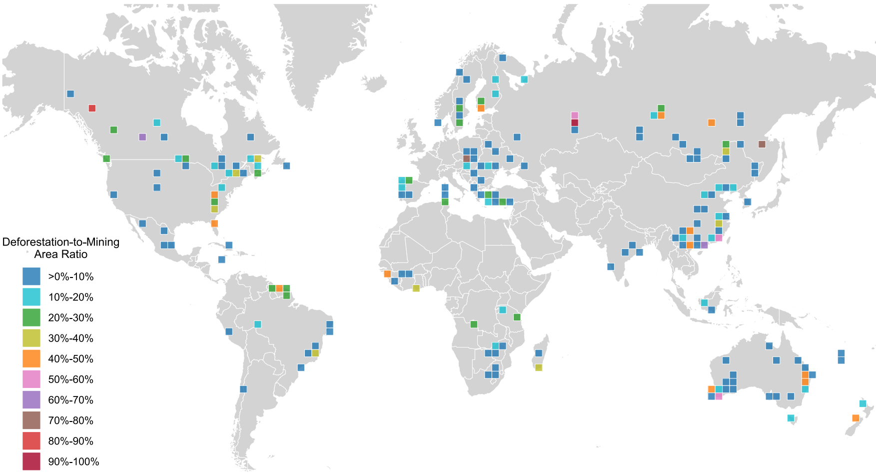

Lithium

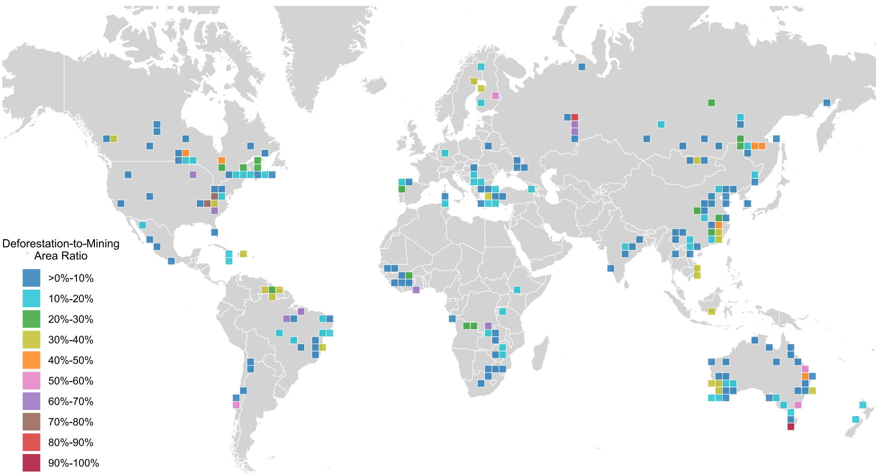

PGE

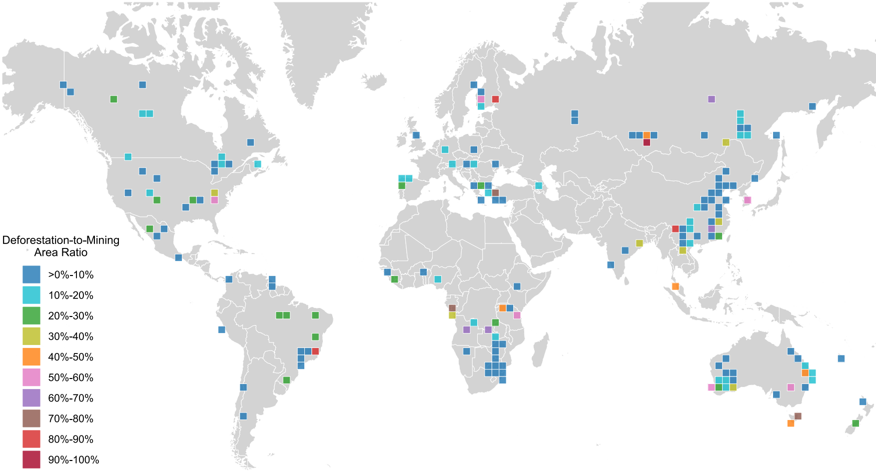

Uranium

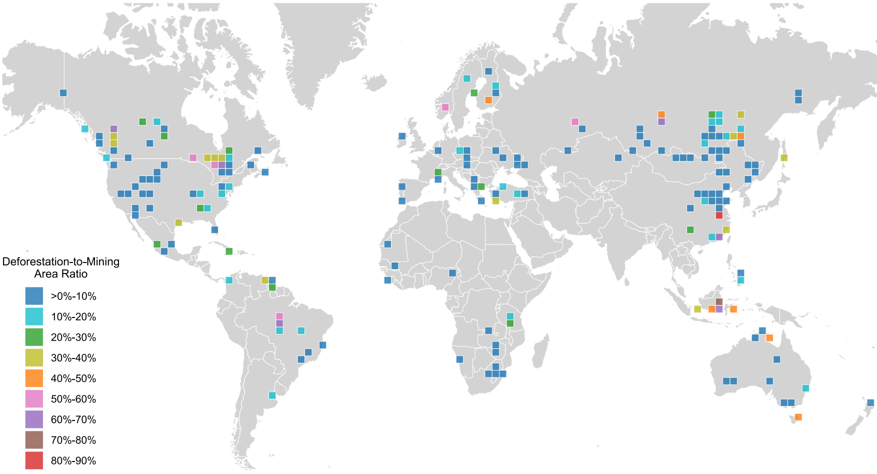

Other metals

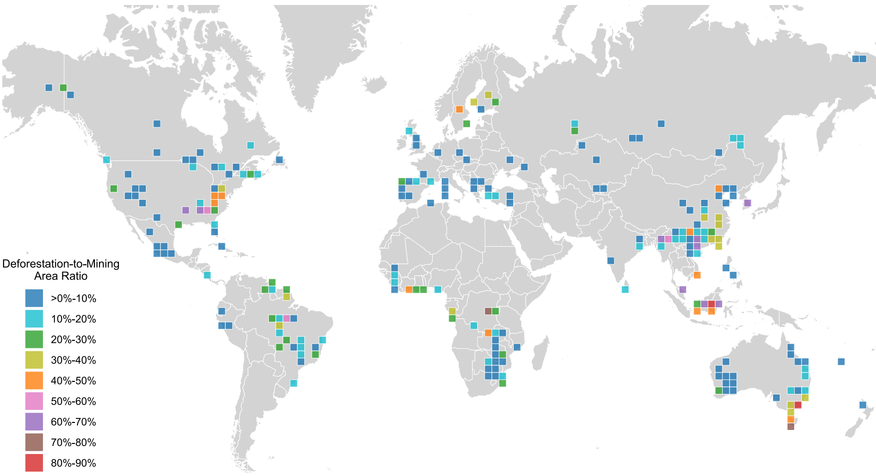

Coal

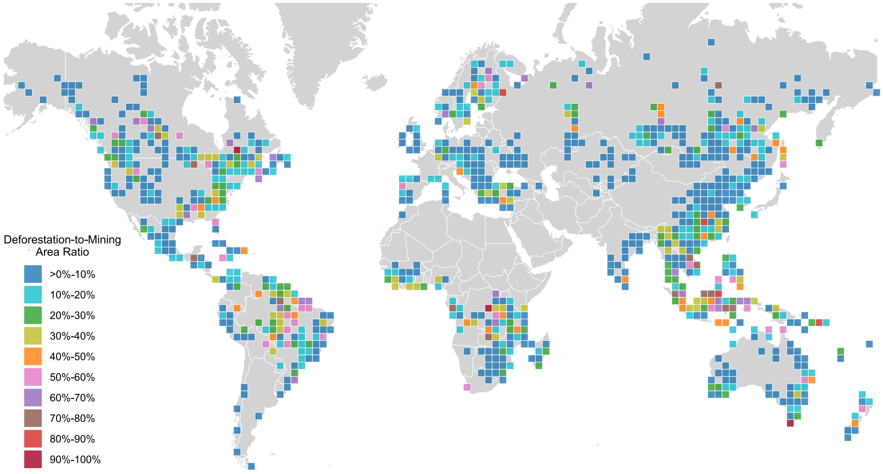

Other non-metals

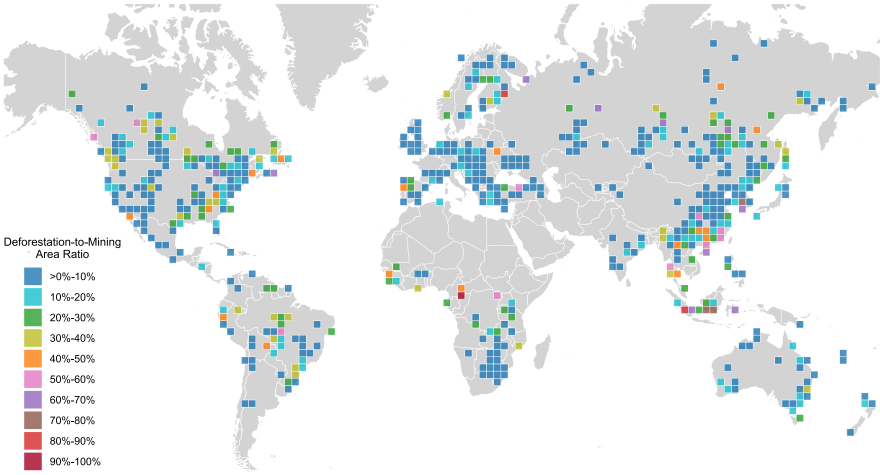

S4. Region-Commodity Combination

Commodity	Deforestation area of countries intersecting the Amazon and Southeast Asian rainforests (% of the total deforestation)	Deforestation area of other countries (% of the total deforestation)
Iron	418.69 (2.86%)	627.32 (4.29%)
Gold	2123.16 (14.52%)	1060.49 (7.25%)
Nickel and Cobalt	271.79 (1.86%)	345.00 (2.36%)
Aluminium (Bauxite)	432.76 (2.96%)	331.95 (2.27%)
Coal	4147.95 (28.37%)	1896.80 (12.97%)
Others	776.10 (5.31%)	2187.04 (14.96%)
ALL	8170.45 (55.89%)	6448.60 (44.11%)

S5. Spatial Variation in Extinction Risk Index (ERI) for 20 Commodities

Iron

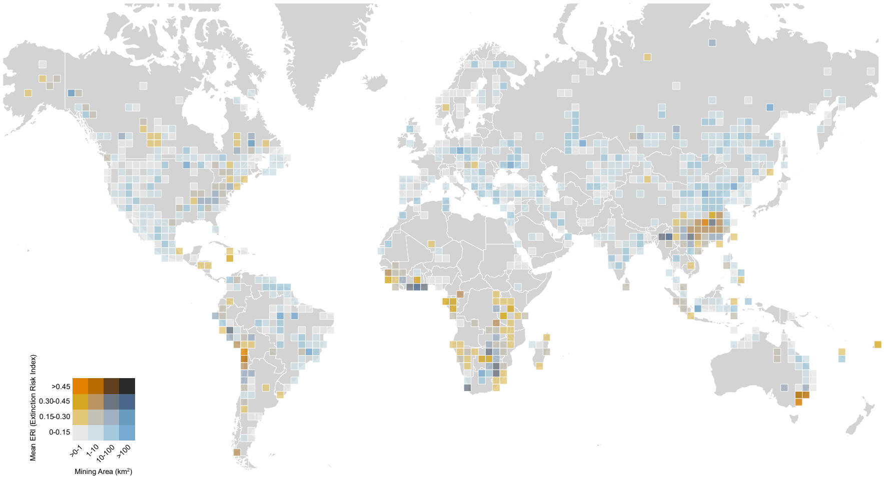

Copper

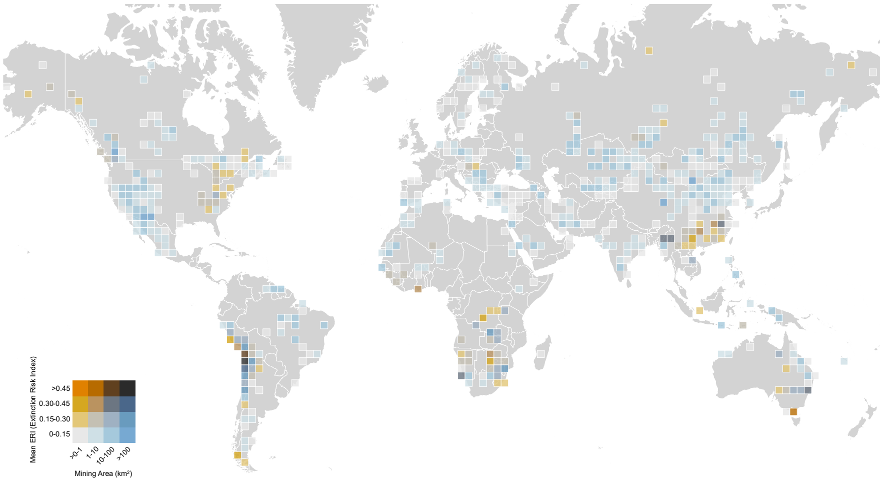

Lead

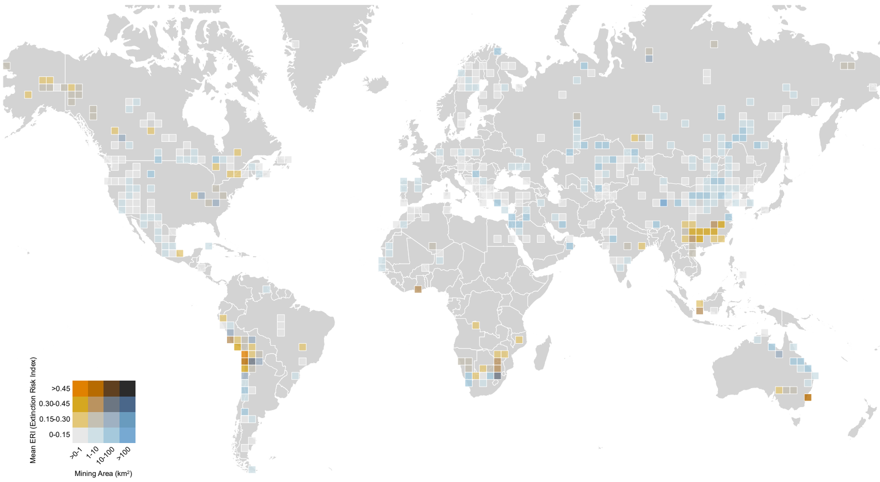

Zinc

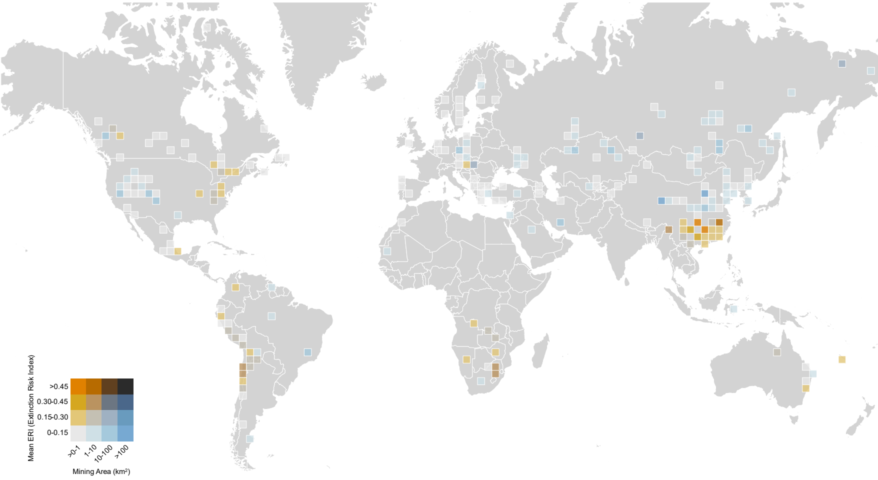

Gold

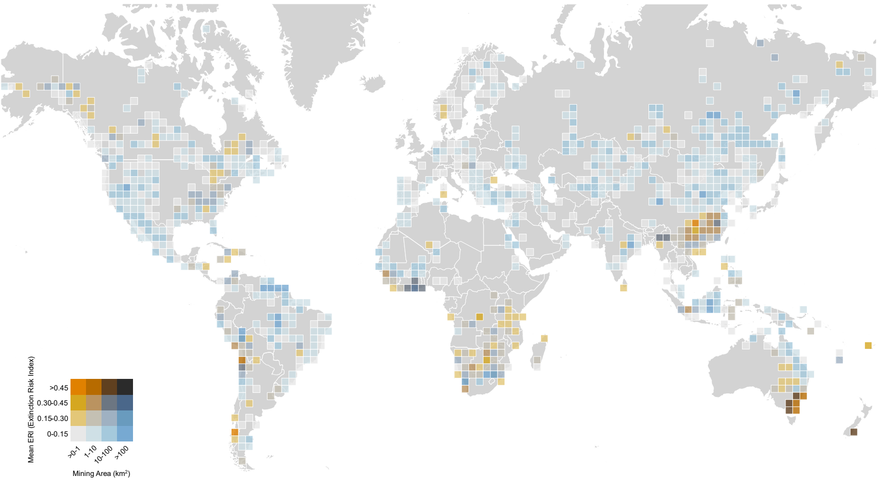

Silver

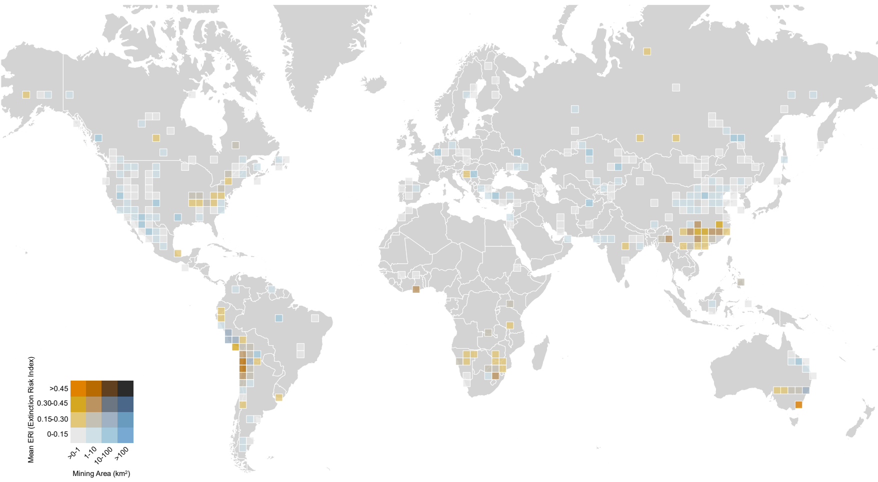

Chromium

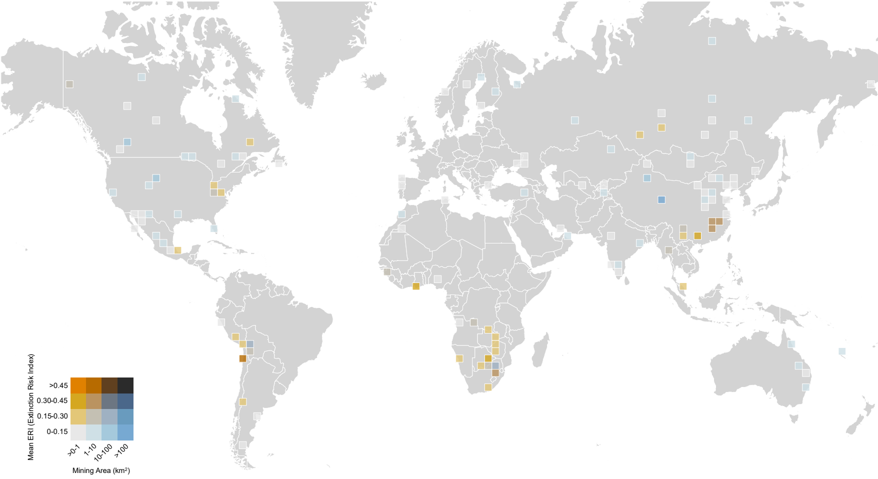

Manganese

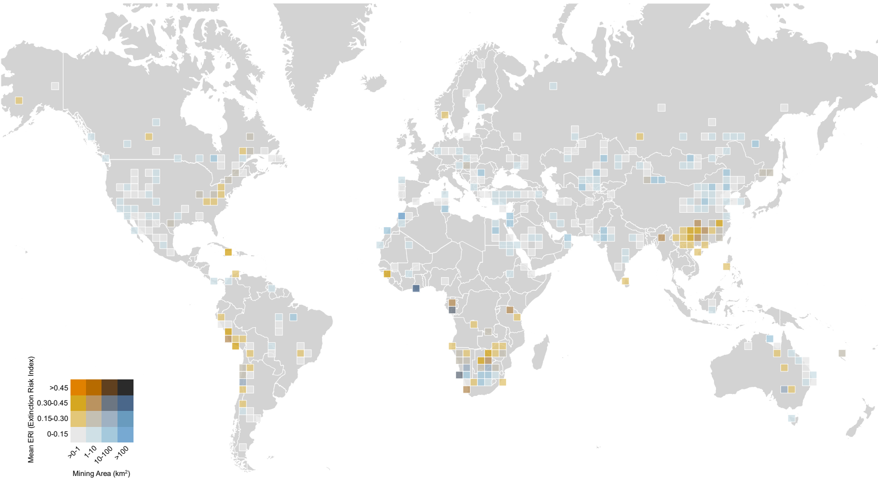

Molybdenum

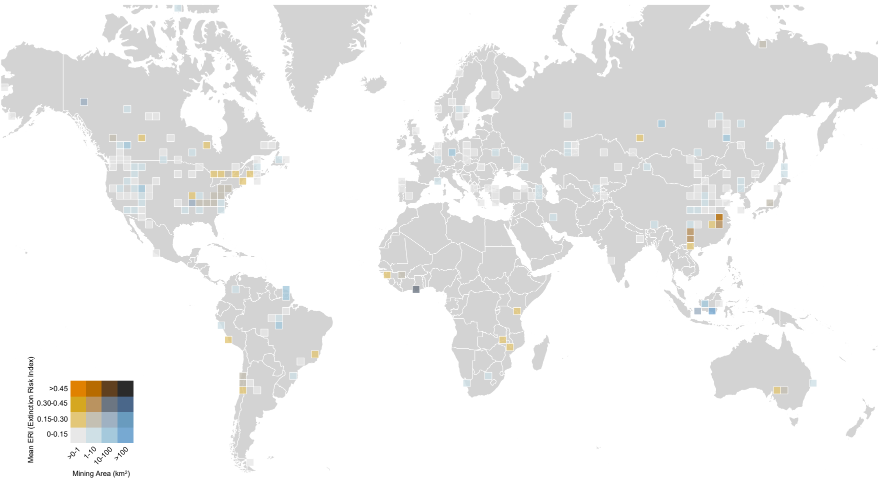

Nickel and Cobalt

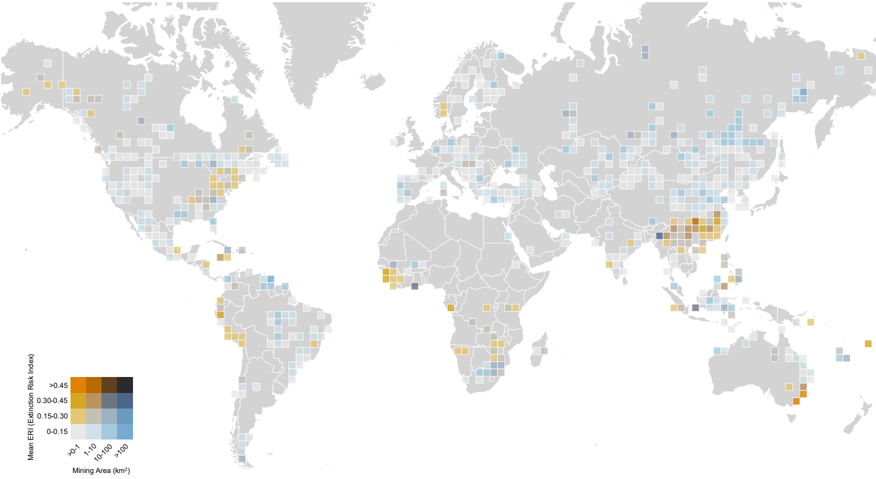

Tin

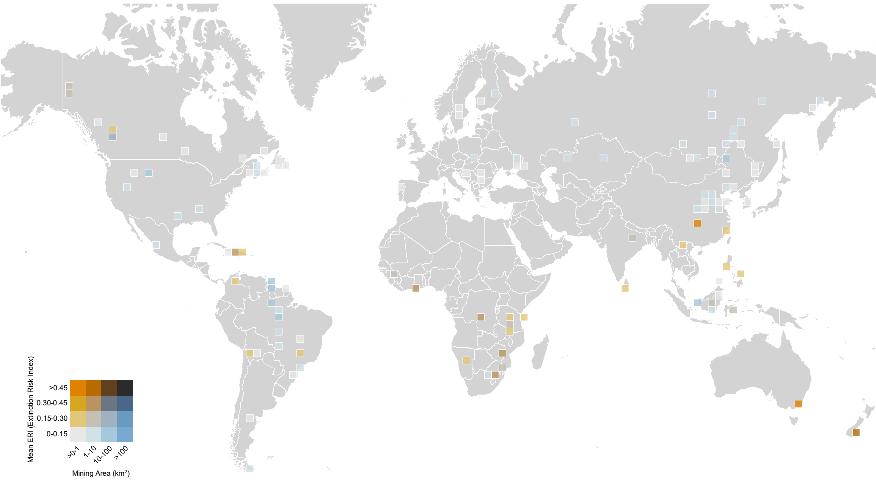

Tungsten

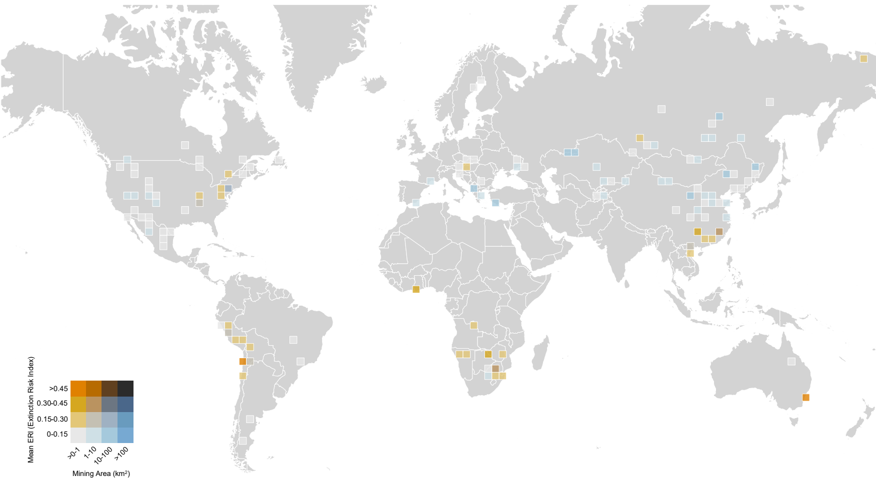

Aluminium (Bauxite)

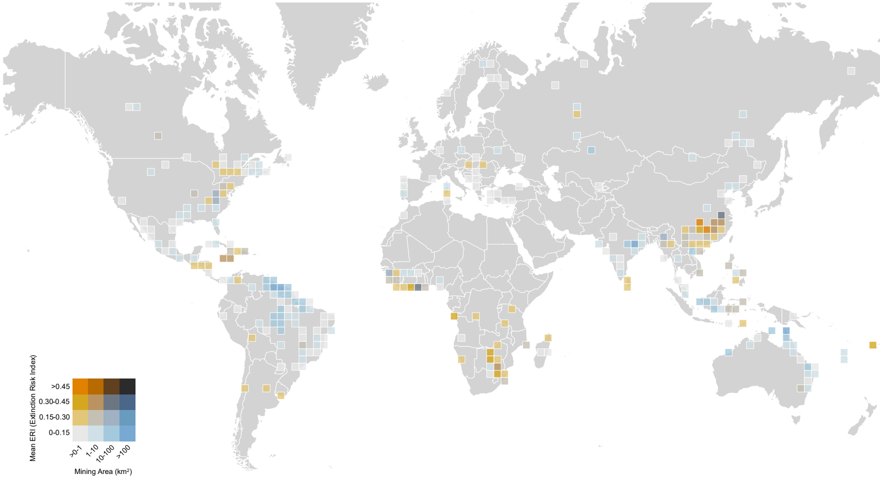

Ilmenite

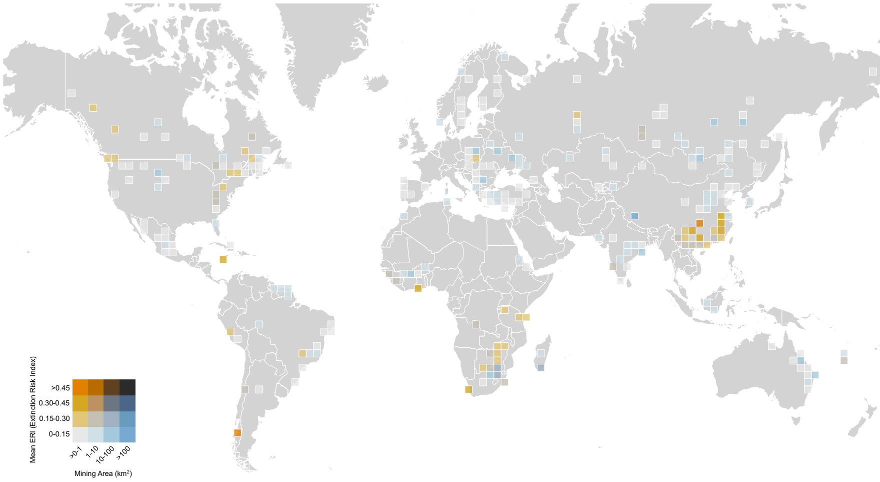

Lithium

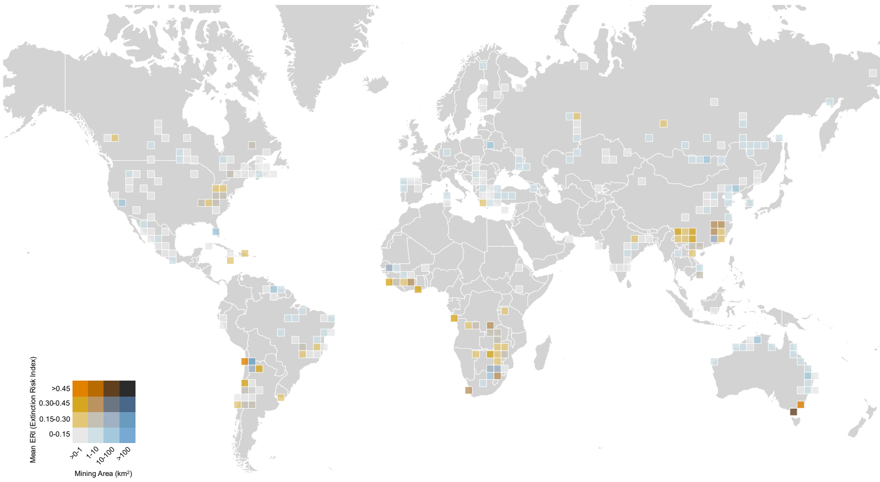

PGE

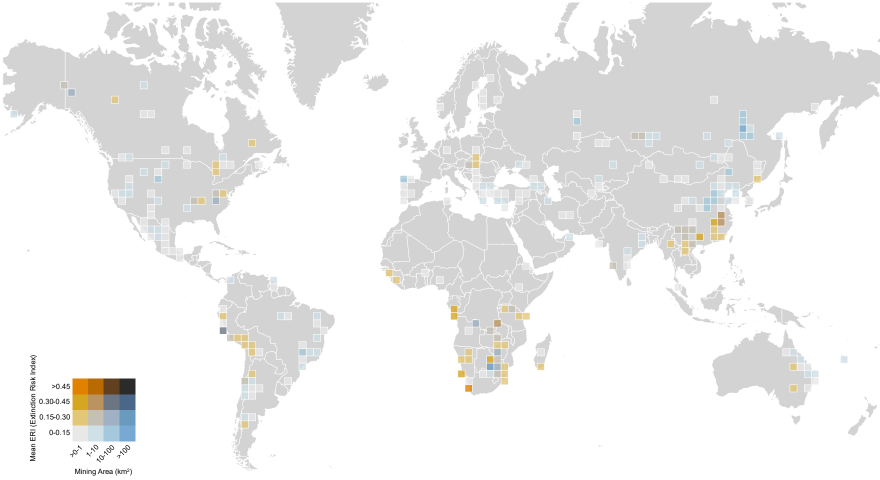

Uranium

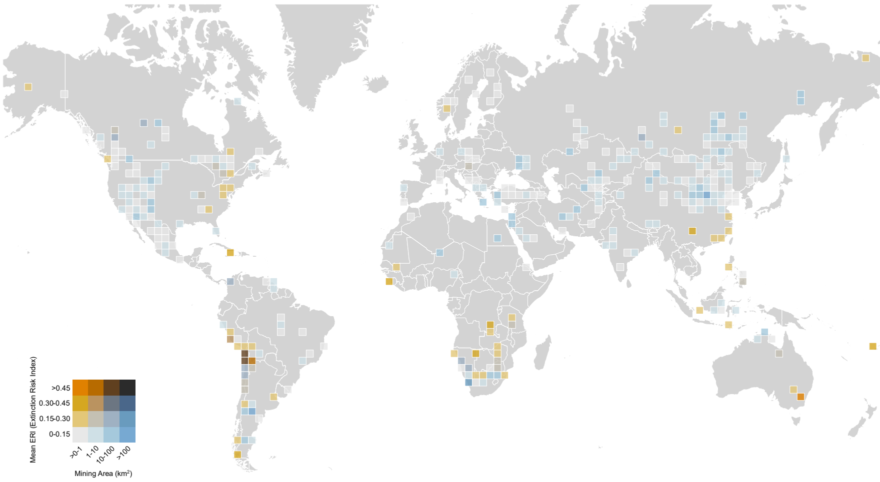

Other metals

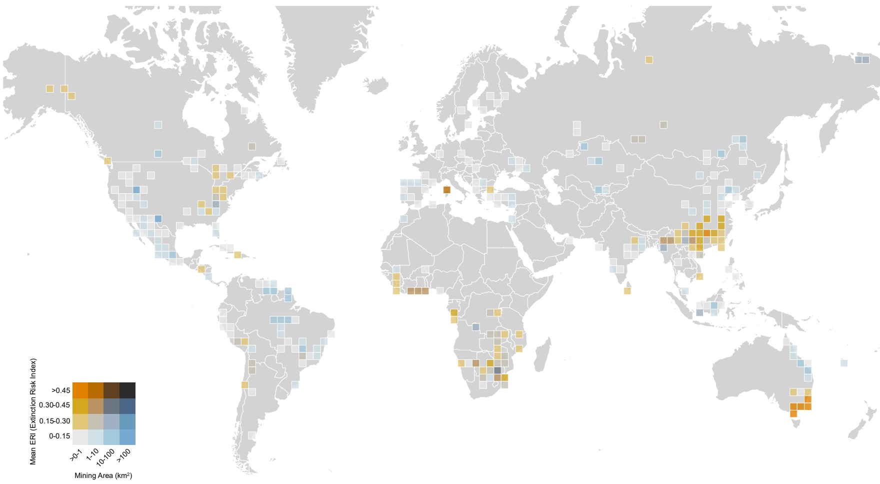

Coal

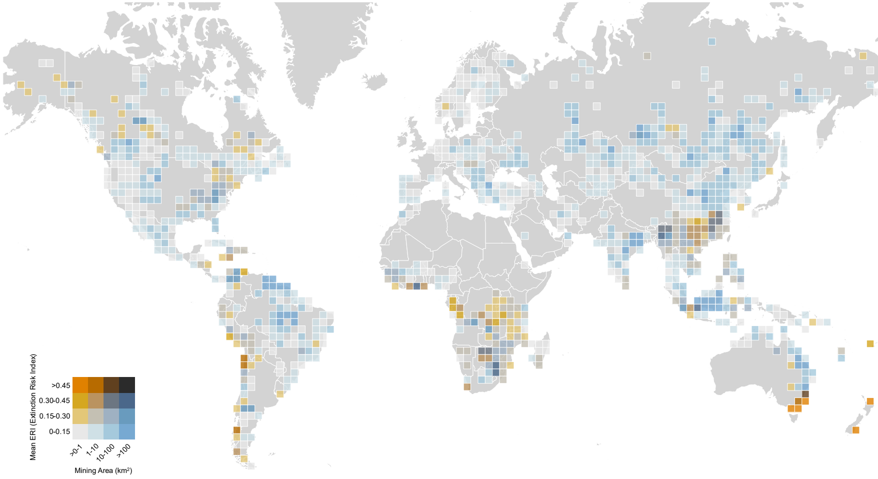

Other non-metals

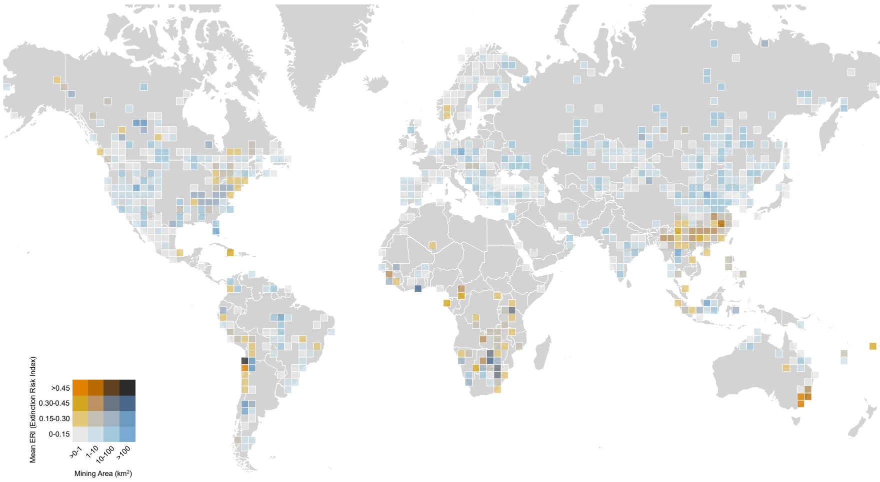

S6. Data Sources and Preparation

This study's commodity classification builds on the delineation of mining areas from Maus *et al.*[1,2]. The dataset, consisting of 44,929 polygons covering 101,583 km², represents a range of mining activities. However, as the Maus *et al.*[2] dataset lacks detailed commodity information, we supplemented it with point data from sources such as the SNL metals & mining dataset[3], USGS[4], Jasansky *et al.*[5], and Franks *et al.*[6], all of which provide spatial coordinates and commodity details. A spatial join was performed to integrate these point datasets with Maus *et al*'s polygons[2], linking point data to polygons where spatial overlap was detected. In cases where multiple points were associated with a single polygon, the most frequently represented commodity was assigned, and where no clear majority existed, a commodity was randomly selected. This process successfully labelled 1,941 polygons with commodity information into 20 commodity classes (see Table S6).

Table S6 shows that the 1,941 labelled polygons cover 30,890.83 km², representing about 4% of the polygons in the Maus *et al.* dataset[2] but accounting for nearly 30% of the total land area. This suggests that larger industrial mines, which are more likely to be documented, are disproportionately represented, while smaller operations may be underreported. Gold is the most prevalent commodity by both polygon count and area, reflecting its economic importance and the availability of reliable data. However, some larger polygons may include non-mining areas, as noted by Tang and Werner[7]; for instance, one gold polygon spans 2,546 km², nearly covering the entire upstream region of the Rio Madre De Dios River in Chile. Despite such limitations, the Maus *et al.* dataset[2] remains valuable for global commodity classification.

Table S6 - Distribution of Mineral Categories after initial data integration

Commodity	Number of Polygons (% of Polygons)	Covered Areas (% of Covered Areas)
Iron	195 (10.046%)	3074.230 (9.95%)
Copper	264 (13.601%)	4564.758 (14.78%)
Lead	26 (1.340%)	155.419 (0.50%)
Zinc	93 (4.791%)	314.733 (1.02%)
Gold	528 (27.202%)	8429.676 (27.29%)
Silver	57 (2.937%)	169.185 (0.55%)
Chromium	12 (0.618%)	51.436 (0.17%)
Manganese	13 (0.670%)	142.978 (0.46%)
Molybdenum	13 (0.670%)	137.116 (0.44%)
Nickel and Cobalt	64 (3.297%)	560.869 (1.82%)
Tin	4 (0.206%)	87.531 (0.28%)
Tungsten	5 (0.258%)	4.470 (0.01%)
Aluminium (Bauxite)	42 (2.164%)	928.334 (3.01%)
Ilmenite	7 (0.361%)	70.116 (0.23%)
Lithium	7 (0.361%)	65.408 (0.21%)
PGE	34 (1.752%)	169.852 (0.55%)
Uranium	26 (1.340%)	227.621 (0.74%)
Other metals	15 (0.773%)	326.109 (1.06%)
Coal	386 (19.887%)	7224.282 (23.39%)
Other non-metals	150 (7.728%)	4186.712 (13.55%)
Total	1941 (100%)	30890.834 (100%)

S7. Open-pit Identification

Before classifying commodities for polygons without labels, a machine-learning model was developed using a random forest algorithm to detect open pits within each mining area polygon. Random forests are widely regarded for classification tasks, particularly for their robustness in handling high-dimensional datasets and their resistance to overfitting[8]. 558 ASTER scenes were used and filtered to remove areas containing snow, clouds, and water bodies according to criteria established by Hall *et al.*[9], Werner *et al.*[10], and the JRC Monthly Water History dataset[11]. Vegetative interference was minimised by selecting scenes with the lowest band values, ensuring more reliable spectral analysis and reducing environmental noise.

The model was trained using an 80:20 cross-validation approach, splitting the scenes into training and validation subsets. Table S7.1 details the distribution of land-use types across these subsets. "Open Pit" and "Vegetation" classes have the most samples, reflecting their prevalence in real-world mining regions. In contrast, the "Dam" and "Waste Rock Dump (WRD)" classes contain fewer samples, consistent with their less frequent occurrence. This distribution reflects the true environmental heterogeneity in mining areas, ensuring the model is trained to represent realistic conditions, thus improving the generalisability of its predictions.

The model's performance is summarised in Table S7.2, which presents the confusion matrix for open-pit identification along with accuracy metrics. The model achieved an overall accuracy of 87.76%, with open pits correctly classified in 25 of 27 instances (92.6% accuracy). In addition, the model successfully identified dams, WRD, and facilities in 23 of 30 instances (76.7% accuracy). These results validate the model's utility in identifying critical mining infrastructure across diverse land-use types.

Table S7.1 – Distribution of Training and Validation Subsets for Open-pit Identification

Land Use	Training Subset	Validation Subset
Open Pit	97	27
Dam	35	7
Waste Rock Dump	63	9
Facility	81	14
Vegetation	100	23
Bare Soil	84	18

Table S7.2 – Confusion Matrix for Open-Pit Identification

Land Use	Open Pit	Dam	Waste Rock Dump	Facility	Vegetation	Bare Soil	User's accuracy
Open Pit	25	1	0	0	1	0	92.59%
Dam	1	5	0	0	1	0	71.43%
Waste Rock Dump	0	1	6	0	1	1	66.67%
Facility	0	0	2	12	0	0	85.71%
Vegetation	1	0	0	1	20	1	86.96%
Bare Soil	0	0	0	0	0	18	100.00%
Producer's accuracy	92.59%	71.43%	75.00%	92.31%	86.96%	90.00%	Overall: 87.76%

S8. Commodity Classification

Following identifying open-pit points for each polygon, a commodity classification model was applied to assign the appropriate commodities to each point corresponding to its respective polygon. The model was based on 26 band ratio indices derived from the ASTER Mineral Index Processing Manual[12], as outlined in Table S8.1. The distribution of training and validation subsets used for the classification process is detailed in Table S8.2. Confusion matrices summarising the performance of the commodity classification are shown in Table S8.3, while the overall confusion matrix and user's and producer's accuracies are presented in Tables S8.4 and S8.5. The final classification outcomes are provided in Table S8.6.

Among the 20 commodities, iron, copper, lead, zinc, nickel-cobalt, and coal were validated using external mine site datasets, including iron from the Global Iron Ore Mines Tracker[13], coal from the Global Coal Mine Tracker[14], and copper, lead-zinc, and nickel datasets from Northey *et al.*[15], which provide coordinate points but lack mining boundary and area information. All external datasets encompass mines with various statuses, such as operating, mothballed, proposed, or retired. In addition, the two Tracker datasets[13,14] provide location accuracies classified as exact or proximate, while the Global Coal Mine Tracker[14] uniquely includes information on mine type, distinguishing between surface and underground mines.

In this context, only operating mines were included. Specifically, for iron and coal, only mines with exact location accuracy were used, and only surface coal mines were considered. The validation accuracies for these commodities, presented in Table S8.7, are based on the number of points that intersect with the polygons (Table S8.6) and the areas of these intersecting polygons. Notably, each polygon in this study is assigned a primary commodity. As a result, cases such as an iron mine point intersecting with a copper polygon identified from other sources[3,4,5,6,13,14,15] can occur (e.g. Iron Oxide Copper-Gold deposits). These instances are not deemed incorrect but are recognised as valid due to the multi-commodity nature of mining areas. Given the limited availability of external datasets, the validation results are considered reasonable and reflect the inherent complexity of mining operations.

Table S8.1 – Band Ratio Indices (Geoscience Australia, 2004)

No.	Indices	Ratio
1	Ferric iron, Fe^{3+}	2/1
2	Ferrous iron, Fe^{2+}	5/3+1/2
3	Laterite/Silica Alteration	4/5
4	Gossan	4/2
5	Ferrous silicates (biot, chi, amph)	5/4
6	Ferric oxides	4/3
7	Carbonate/chlorite/epidote	(7+9)/8
8	Epidote/chlorite/amphibole	(6+9)/(7+8)
9	Amphibole/MgOH	(6+9)/8
10	Amphibole	6/8
11	Dolomite	(6+8)/7
12	Carbonate	13/14
13	Sericite/muscovite/illite/smectite	(5+7)/6
14	Alunite/kaolinite/pyrophyllite	(4+6)/5
15	Phengitic/Host rock	5/6
16	Muscovite	7/6
17	Kaolinite	7/5
18	Clay	$(5x7)/6^2$
19	Quartz rich rocks	14/12
20	Silica (1)	(11x11)/10/12
21	Basic degree index (gnt, cpx, epi, chl)/SiO_2	12/13
22	SiO_2	13/12
23	Siliceous rocks	(11x11)/(10x12)
24	Silica (2)	11/10
25	Silica (3)	11/12
26	Silica (4)	13/10

Table S8.2a – Distribution of Training and Validation Subsets for Commodity Classification (Level 1)

Commodity	Training Subset	Validation Subset
Non-metals	1248	312
Non-iron metals	1297	325
Iron	1297	325

Table S8.2b – Distribution of Training and Validation Subsets for Commodity Classification (Level 2-1)

Commodity	Training Subset	Validation Subset
Other non-metals	416	104
Coal	416	104

Table S8.2c – Distribution of Training and Validation Subsets for Commodity Classification (Level 2-2)

Commodity	Training Subset	Validation Subset
Chalcophile-related metals	416	104
Aluminium (Bauxite)	416	104
Chromium	416	104
Nickel and Cobalt	416	104
Lithium	416	104
Manganese	416	104
Other metals	416	104
PGE	416	104
Tin	416	104
Ilmenite	416	104
Tungsten	416	104
Uranium	416	104

Table S8.2d – Distribution of Training and Validation Subsets for Commodity Classification (Level 3-1)

Commodity	Training Subset	Validation Subset
Copper	416	104
Gold	416	104
Lead	416	104
Molybdenum	416	104
Silver	416	104
Zinc	416	104

Table S8.3a – Confusion Matrix for Commodity Classification (Level 1)

	Non-metals	Non-iron metals	Iron
Non-metals	253	59	10
Non-iron metals	40	230	2
Iron	19	36	313

Table S8.3b – Confusion Matrix for Commodity Classification (Level 2-1)

	Other non-metals	Coal
Other non-metals	89	25
Coal	15	79

Table S8.3c – Confusion Matrix for Commodity Classification (Level 2-2)

	Chalco-phile-related metals	Alu-minium (Bauxite)	Chro-mium	Cobalt and Nickel	Lith-ium	Manga-nese	Other metals	PGE	Tin	Il-menite	Tung-sten	Ura-nium
Chalcophile-related metals	67	1	1	1	0	0	0	1	0	0	0	0
Aluminium (Bauxite)	5	103	0	0	0	0	0	0	0	0	0	0
Chromium	1	0	101	0	0	1	2	0	0	0	0	0
Nickel and Cobalt	9	0	0	98	0	9	0	1	0	0	0	0
Lithium	1	0	0	0	104	1	0	0	0	0	0	0
Manganese	3	0	0	1	0	100	0	1	1	0	0	0
Other metals	6	0	0	1	0	6	102	0	0	0	0	0
PGE	2	0	2	1	0	2	0	101	0	0	0	1
Tin	2	0	1	0	0	0	0	0	103	0	0	0
Ilmenite	2	0	0	1	0	2	0	0	0	104	0	0
Tungsten	2	0	0	1	0	0	0	0	0	0	104	1
Uranium	6	0	0	0	0	0	0	0	0	0	0	101

Table S8.3d – Confusion Matrix for Commodity Classification (Level 3-1)

	Copper	Gold	Lead	Molybdenum	Silver	Zinc
Copper	69	21	1	0	0	3
Gold	19	69	9	1	0	0
Lead	8	5	84	0	4	2
Molybdenum	1	3	0	102	1	0
Silver	3	5	8	0	98	0
Zinc	4	1	2	1	1	99

Table S8.4 Overall Confusion Matrix

	Non-metals	Non-iron Metals	Iron	Other non-metals	Coal	Chalcophile-related metals	Aluminium (Bauxite)	Chromium	Nickel and Cobalt	Lithium	Manganese	Other metals	PGE	Tin	Ilmenite	Tungsten	Uranium	Copper	Gold	Lead	Molybdenum	Silver	Zinc
Non-metals	253	59	10	0	0	0	0	0	0	0	0	0	0	0	0	0	0	0	0	0	0	0	0
Non-iron metals	40	230	2	0	0	0	0	0	0	0	0	0	0	0	0	0	0	0	0	0	0	0	0
Iron	19	36	313	0	0	0	0	0	0	0	0	0	0	0	0	0	0	0	0	0	0	0	0
Other non-metals	0	0	0	89	25	0	0	0	0	0	0	0	0	0	0	0	0	0	0	0	0	0	0
Coal	0	0	0	15	79	0	0	0	0	0	0	0	0	0	0	0	0	0	0	0	0	0	0
Chalcophile-related metals	0	0	0	0	0	67	1	1	1	0	0	0	1	0	0	0	0	0	0	0	0	0	0
Aluminium (Bauxite)	0	0	0	0	0	5	103	0	0	0	0	0	0	0	0	0	0	0	0	0	0	0	0
Chromium	0	0	0	0	0	1	0	101	0	0	1	2	0	0	0	0	0	0	0	0	0	0	0
Nickel and Cobalt	0	0	0	0	0	9	0	0	98	0	9	0	1	0	0	0	0	0	0	0	0	0	0
Lithium	0	0	0	0	0	1	0	0	0	104	1	0	0	0	0	0	0	0	0	0	0	0	0
Manganese	0	0	0	0	0	3	0	0	1	0	100	0	1	1	0	0	0	0	0	0	0	0	0
Other metals	0	0	0	0	0	6	0	0	1	0	6	102	0	0	0	0	0	0	0	0	0	0	0
PGE	0	0	0	0	0	2	0	2	1	0	2	0	101	0	0	0	1	0	0	0	0	0	0
Tin	0	0	0	0	0	2	0	1	0	0	0	0	0	103	0	0	0	0	0	0	0	0	0
Ilmenite	0	0	0	0	0	2	0	0	1	0	2	0	0	0	104	0	0	0	0	0	0	0	0
Tungsten	0	0	0	0	0	2	0	0	1	0	0	0	0	0	0	104	1	0	0	0	0	0	0
Uranium	0	0	0	0	0	6	0	0	0	0	0	0	0	0	0	0	101	0	0	0	0	0	0
Copper	0	0	0	0	0	0	0	0	0	0	0	0	0	0	0	0	0	69	21	1	0	0	3
Gold	0	0	0	0	0	0	0	0	0	0	0	0	0	0	0	0	0	19	69	9	1	0	0
Lead	0	0	0	0	0	0	0	0	0	0	0	0	0	0	0	0	0	8	5	84	0	4	2
Molybdenum	0	0	0	0	0	0	0	0	0	0	0	0	0	0	0	0	0	1	3	0	102	1	0
Silver	0	0	0	0	0	0	0	0	0	0	0	0	0	0	0	0	0	3	5	8	0	98	0
Zinc	0	0	0	0	0	0	0	0	0	0	0	0	0	0	0	0	0	4	1	2	1	1	99

Table S8.5 User's Accuracy and Producer's Accuracy for 20 Commodities

Commodity	User's accuracy	CI lower bound	CI upper bound	Producer's accuracy	CI lower bound	CI upper bound
Iron	85.05%	81.41%	88.70%	96.31%	94.26%	98.36%
Copper	73.40%	64.47%	82.34%	66.35%	57.26%	75.43%
Lead	81.55%	74.06%	89.04%	80.77%	73.19%	88.34%
Zinc	91.67%	86.45%	96.88%	95.19%	91.08%	99.30%
Gold	70.41%	61.37%	79.45%	66.35%	57.26%	75.43%
Silver	85.96%	79.59%	92.34%	94.23%	89.75%	98.71%
Chromium	96.19%	92.53%	99.85%	96.19%	92.53%	99.85%
Manganese	94.34%	89.94%	98.74%	82.64%	75.90%	89.39%
Molybdenum	95.33%	91.33%	99.33%	98.08%	95.44%	100.00%
Nickel and Cobalt	83.76%	77.08%	90.44%	94.23%	89.75%	98.71%
Tin	97.17%	94.01%	100.00%	99.04%	97.16%	100.00%
Tungsten	96.30%	92.73%	99.86%	100.00%	96.52%	100.00%
Aluminium (Bauxite)	95.37%	91.41%	99.33%	99.04%	97.16%	100.00%
Ilmenite	95.41%	91.49%	99.34%	100.00%	96.52%	100.00%
Lithium	98.11%	95.52%	100.00%	100.00%	96.52%	100.00%
PGE	92.66%	87.76%	97.56%	97.12%	93.90%	100.00%
Uranium	94.39%	90.03%	98.75%	98.06%	95.39%	100.00%
Other metals	88.70%	82.91%	94.48%	98.08%	95.44%	100.00%
Coal	84.04%	76.64%	91.45%	75.96%	67.75%	84.17%
Other non-metals	78.07%	70.47%	85.67%	85.58%	78.82%	92.33%

Overall accuracy		
Accuracy	CI lower bound	CI upper bound
87.32%	86.15%	88.50%

Table S8.6a Commodity Classification Result (Polygons)

Commodity	Polygons (n)				Prop (Total)
	Total	Trained	Predicted	Connected	
Iron	5484	195	4946	343	14.29%
Copper	2427	264	1962	201	6.33%
Lead	1182	93	1015	74	3.08%
Zinc	437	13	399	25	1.14%
Gold	5021	528	4219	274	13.09%
Silver	832	57	712	63	2.17%
Chromium	216	12	189	15	0.56%
Manganese	1039	13	963	63	2.71%
Molybdenum	399	26	347	26	1.04%
Nickel and Cobalt	2112	64	1919	129	5.50%
Tin	208	4	183	21	0.54%
Tungsten	187	5	172	10	0.49%
Aluminium (Bauxite)	890	42	810	38	2.32%
Ilmenite	619	7	574	38	1.61%
Lithium	726	7	683	36	1.89%
PGE	766	34	678	54	2.00%
Uranium	925	26	858	41	2.41%
Other metals	721	15	667	39	1.88%
Coal	10553	386	9462	705	27.50%
Other non-metals	3626	150	3303	173	9.45%
ALL	**38370**	**1941**	**34061**	**2368**	**100.00%**

Table S8.6b Commodity Classification Result (Areas)

Commodity	Area (Km^2)				Prop (Total)
	Total	Trained	Predicted	Connected	
Iron	10160.24	3074.23	7006.56	79.45	10.21%
Copper	8429.79	4564.76	3799.22	65.81	8.47%
Lead	2651.65	314.73	2326.16	10.75	2.67%
Zinc	989.25	137.12	848.90	3.23	0.99%
Gold	18143.97	8429.68	9600.91	113.38	18.24%
Silver	920.94	169.18	741.31	10.45	0.93%
Chromium	572.06	51.44	519.95	0.67	0.57%
Manganese	1912.96	142.98	1759.93	10.05	1.92%
Molybdenum	740.22	155.42	572.31	12.49	0.74%
Nickel and Cobalt	4102.65	560.87	3507.94	33.84	4.12%
Tin	462.11	87.53	354.76	19.82	0.46%
Tungsten	364.91	4.47	357.72	2.72	0.37%
Aluminium (Bauxite)	2654.42	928.33	1679.19	46.90	2.67%
Ilmenite	840.60	70.12	766.64	3.84	0.84%
Lithium	1687.42	65.41	1610.74	11.27	1.70%
PGE	1250.69	169.85	1074.19	6.65	1.26%
Uranium	2217.32	227.62	1981.81	7.89	2.23%
Other metals	1534.72	326.11	1198.63	9.98	1.54%
Coal	28948.63	7224.28	21315.80	408.55	29.10%
Other non-metals	10908.44	4186.71	6661.93	59.80	10.96%
ALL	**99492.95**	**30890.83**	**67684.58**	**917.54**	**100.00%**

Table S8.7 External Validation Results for Selected Commodities

Commodity	Mine points (n)			Areas (km^2)		
	Consistent areas	All intersecting points	Accuracy	Consistent areas	All intersecting areas	Accuracy
Iron	175	330	53%	2728	3623	75%
Copper	140	195	72%	3496	3711	94%
Lead-zinc (compared to lead and zinc)	78	113	69%	461	567	81%
Nickel (compared to nickel-cobalt)	125	160	78%	3485	3671	95%
Coal	423	721	59%	6693	9529	70%

References

1. Maus, V. *et al.* A global-scale dataset of mining areas. *Sci. Data* **7**, 289 (2020). https://doi.org/10.1038/s41597-020-00624-w.
2. Maus, V. *et al.* An update on global mining land use. *Sci. Data* **9**, 433 (2022). https://doi.org/10.1038/s41597-022-01547-4.
3. S&P Global Market Intelligence. SNL metals & mining data. (2023).
4. U.S. Geological Survey. Major mineral deposits of the world: Regional locations and general geologic setting of known deposits of major nonfuel mineral commodities [Dataset]. (2005). https://mrdata.usgs.gov/services/ofr20051294.
5. Jasansky, S., Lieber, M., Giljum, S. & Maus, V. An open database on global coal and metal mine production. *Sci. Data* **10**, 52 (2023).
6. Franks, D. M. *et al.* Tailings facility disclosures reveal stability risks. *Sci. Rep.* **11**, 5353 (2021). https://doi.org/10.1038/s41598-021-84722-w.
7. Tang, L. & Werner, T. T. Global mining footprint mapped from high-resolution satellite imagery. Commun. *Earth Environ.* **4**, 134 (2023). https://doi.org/10.1038/s43247-023-00691-6.
8. Breiman, L. Random forests. *Mach. Learn.* **45**, 5–32 (2001).
9. Hall, D. K., Riggs, G. A. & Salomonson, V. V. Development of methods for mapping global snow cover using Moderate Resolution Imaging Spectroradiometer data. *Remote Sens. Environ.* **54**, 127–140 (1989).
10. Werner, F. *et al.* Marine boundary layer cloud property retrievals from high-resolution ASTER observations: case studies and comparison with Terra MODIS. *Atmos. Meas. Tech.* **9**, 5869–5894 (2016). https://doi.org/10.5194/amt-9-5869-2016.
11. Pekel, J.-F., Cottam, A., Gorelick, N. & Belward, A. S. High-resolution mapping of global surface water and its long-term changes. *Nature* **540**, 418–422 (2016). https://doi.org/10.1038/nature20584.

12. Kalinowski, A. & Oliver, S. ASTER mineral index processing manual. (Geoscience Australia, 2004). https://www.ga.gov.au/bigobj/GA7833.pdf.

13. Global Energy Monitor. Global Iron Ore Mines Tracker (V1). November 2024. Available at: https://globalenergymonitor.org.

14. Global Energy Monitor. Global Coal Mine Tracker. April 2024 release. Global Energy Monitor, 2024. Available at: https://globalenergymonitor.org.

15. Northey, S. A., Mudd, G. M., Werner, T. T., Jowitt, S. M., Haque, N., Yellishetty, M., & Weng, Z. The exposure of global base metal resources to water criticality, scarcity and climate change. *Global Environmental Change* **44**, 109–124 (2017). https://doi.org/10.1016/j.gloenvcha.2017.04.004.